Core Ionization Energies, Mean Dipole Moment Derivatives, and Simple Potential Models for B, N, O, F, P, Cl, and Br Atoms in Molecules

Roberto L. A. Haiduke, Anselmo E. de Oliveira, and Roy E. Bruns*

Instituto de Química, Universidade Estadual de Campinas, CP 6154, 13083-970 Campinas, SP, Brazil

Received: September 20, 2001; In Final Form: December 28, 2001

Simple potential models relating experimental 1s electron ionization energies for B, N (sp and sp^3 hybrids), O, and F atoms; 1s and 2p ionization energies for P atoms; and 2s and 2p ionization energies for Cl atoms as a function of their atomic mean dipole moment derivatives determined from experimental gas phase infrared fundamental band intensities are reported. Potential models using theoretical Koopmans' energies and generalized atomic polar tensor (GAPT) charges are found to form even more precise models than those using experimental data. This is expected because the potential models depend only on the electronic structures of molecules before ionization takes place and do not take into account relaxation effects. If the experimental ionization energies are adjusted by their relaxation energies, models similar to those obtained using Koopmans' energies are determined. The models permit a simple understanding of substituent effects on core ionization energies in terms of atomic charges in molecules. Most of the potential model slopes investigated are shown to be approximately proportional to the inverse atomic radii of the atom being ionized. Core-valence electron repulsion values inferred from the potential models obtained from experimental data are somewhat smaller than those calculated using Slater orbitals of isolated atoms. The potential model intercepts for 1s and 2p electrons are shown to be proportional to the square of the nuclear charge, consistent with their interpretation as core electron ionization energies of neutral atoms. 1s He, Ne, and Ar and 2p Ar, Kr, and Xe core ionization energies obey the linear relationships obtained for the model intercepts. The results suggest that mean dipole moment derivatives obtained from infrared intensities can be interpreted as atomic charges.

Introduction

Recently our research group has shown that simple potential models[1] relate core electron ionization energies determined by X-ray photoelectron spectroscopy to mean dipole moment derivatives evaluated from experimental measurements of fundamental gas-phase infrared intensities for a large group of carbon atom containing molecules.[2] The carbon 1s electron ionization energy, $E_{C,1s}$, can be expressed as

$$E_{C,1s} = k_C \bar{p}_C + \sum_{A \neq C} \left(\frac{\bar{p}_A}{R_{AC}} \right) + E_{relax} + E_{0,C} \qquad (1)$$

where $\bar{p}_C$ and $\bar{p}_A$ are mean dipole moment derivatives of the carbon atom that is being ionized and another atom, *A*, that is not involved in the ionization process. R_{AC} is the internuclear distance between these atoms. The sum in the above equation is taken over all of the atoms in the molecule except the ionizing atom and this term represents the electrostatic potential that the neighboring atoms in the molecule create at the atomic nucleus of the atom being ionized. The relaxation energy, E_{relax}, corresponds to the energy released when the remaining electronic density reorganizes to adapt itself to the new situation of an electron hole in the 1s orbital of the ion. The constant, k_C, has been shown to depend on the hybridization state of the carbon atom being ionized with separate models found for the sp^3, sp^2, and sp hybridized carbon atoms. $E_{0,C}$ is a constant equal to the intercept of the $E_{C,1s}$ vs $\bar{p}_C$ line after the neighboring atom electrostatic potential and relaxation energies have been discounted from the experimental ionization energy.

Later, it was shown that this simple potential model was also adequate to represent the np core ionization energies of the group IV Si, Ge, and Sn atoms.[3] Although experimentally determined core electron ionization energies and infrared fundamental gas phase intensities are limited for Si, Ge, and Sn containing molecules, molecular orbital calculations of Koopmans' energies or ΔSCF ionization energies corrected by associated relaxation energies were used to supplement the experimental data. In fact, Koopmans' energies are extremely simple to calculate because they are just the negatives of the molecular orbital energies from Hartree−Fock calculations. Furthermore, they are highly appropriate for simple potential model calculations because this model, like the Koopmans' energies, does not take into account relaxation effects that are extremely important for estimating experimental ionization energies using molecular orbital methods.[4]

It is the main purpose of this paper to show that the simple potential model, evaluated using infrared intensity parameters, is also applicable to core ionization energies of electrons associated with atoms of chemical groups other than group IV. Mean dipole moment derivatives of molecules containing B, N, O, F, P, and Cl atoms are related to core electron ionization energies of these atoms via the simple potential model. Infrared fundamental intensities in the gas phase have been measured for very few molecules containing B and P atoms. As such, potential models are investigated for them using the available

* To whom correspondence should be addressed. E-mail: bruns@iqm.unicamp.br.

10.1021/jp013587s CCC: $22.00
Published on Web 02/08/2002

experimental ionization energies and mean dipole moment derivatives supplemented by theoretical derivatives and Koopmans' energies calculated from ab initio wave functions. For all of the other atoms listed above, potential models can be determined using only experimental data although models are also obtained from theoretical results for comparison purposes. Because relatively few experimental gas phase infrared intensity determinations are reported in the literature and it was decided that this study be restricted mostly to molecules for which experimental results are available, this report is limited to the atoms listed above and to the bromine atom because its results can be compared with those for molecules containing fluorine and chlorine atoms. However, complementary studies could be made on a wider variety of atoms if only theoretical results were used.

Characteristics of the different potential models are also studied to permit a detailed understanding of why these models work. The dependence of the slope of these models, *k*, is studied as a function of the covalent radius of the atom that is ionized. Its value is expected to be proportional to the inverse radius because *k* represents an averaged electrostatic interaction of an electron in a core orbital and an electron in a valence orbital. This was indeed found to be true for the group IV atoms.[3] It is of interest to see if this relationship is also valid for atoms containing lone pair electrons or for atoms that do not obey the octet electron rule. For the N atom, sufficient X-ray and infrared data are available so that the effect of different hybridization states of the ionized atom can be assessed. Furthermore the physical interpretation of the $E_{0,C}$ constant will be discussed in the light of the values determined here for the different potential models.

Simple potential model results suggest that atomic mean dipole moment derivatives can be identified with atomic charges that are capable of reproducing electrostatic potentials at the nuclei of molecules.[4,5] Further studies have shown that mean dipole moment derivatives obtained from experimental intensities adequately describe changes in charge quantities with changes in electronegativities of neighboring atoms, hybridization, and other chemical valency parameters.[6] Furthermore, the results of their calculation from quantum chemical wave functions are often called GAPT charges and have been shown to be relatively invariant to basis set changes.[7] Recently, MP2/6-311++G(3d,3p) GAPT charges have been shown to be in agreement, within 0.046 *e*, with 83 mean dipole moment derivatives determined from experimental intensity data.[6] No other type of charge used in chemistry is so closely related to an experimentally measurable quantity and can be determined in such a straightforward manner.

Calculations

Nitrogen, oxygen, fluorine, phosphorus, chlorine, and boron 1s electron ionization energies were taken from the collection of X-ray ionization energies published by Jolly and co-workers.[8] Mean dipole moment derivatives obtained from experimental infrared intensity data and used here have been reported by a number of research groups: $BF_3$and BCl_3;[9] NH_3 and PH_3;[10] NF_3 and PF_3;[11] HCN, C_2N_2, and CH_3CN;[12] NO, CO, NaF, LiF, HCl, and HF;[13] F_2CO and Cl_2CO;[14] H_2CO;[15] Br_2CO;[16] SiF_4;[3] F_2CS;[14] CHF_3, CH_2F_2, CH_3F, CH_3Cl, CH_2Cl_2, and $CHCl_3$;[8] CF_3Cl, CF_2Cl_2, and $CFCl_3$;[17] *cis*-$C_2H_2Cl_2$;[18] CCl_4;[19] ClCN, BrCN, N_2O, OCS, and CO_2;[20] C_6F_6;[21] 1,1-$C_2H_2F_2$;[22] and CF_3I.[23]

Within the harmonic oscillator−linear dipole moment approximations the measured fundamental infrared intensity, A_i, is proportional to the square of the dipole moment derivative with respect to its associated normal coordinate, Q_i

$$A_i = \frac{N_A \pi}{3c^2}\left(\frac{\partial \vec{p}}{\partial Q_i}\right)^2 \qquad i = 1, 2, ..., 3N - 6 \tag{2}$$

with N_A and c being Avogadro's number and the velocity of light.[24] The dipole moment derivatives can be transformed to atomic Cartesian coordinates using the expression[25,26]

$$\mathbf{P}_X = \mathbf{P}_Q \cdot \mathbf{L}^{-1} \cdot \mathbf{U} \cdot \mathbf{B} + \mathbf{P}_\rho \cdot \beta \tag{3}$$

where $\mathbf{P}_Q$ is a $3 \times 3N - 6$ matrix of dipole moment derivatives obtained from measured infrared intensities and $\mathbf{L}^{-1}$, $\mathbf{U}$, and $\mathbf{B}$ are well-known transformation matrixes commonly used in normal coordinate analysis.[27] The $\mathbf{P}_\rho \cdot \beta$ product provides the rotational contributions to the polar tensor elements. As such, the polar tensor elements contained in $\mathbf{P}_X$ are obtained using the molecular geometry (the $\mathbf{B}$ and β matrixes), symmetry (the $\mathbf{U}$ matrix), vibrational frequencies and atomic masses (the normal coordinate $\mathbf{L}^{-1}$ matrix), and permanent dipole moment values ($\mathbf{P}_\beta$ matrix), as well as the experimentally measured intensities.

The molecular polar tensor, $\mathbf{P}_X$, is a juxtaposition of the atomic polar tensors (APTs)

$$\mathbf{P}_X = \{\mathbf{P}_X^{(1)} \cdot \mathbf{P}_X^{(2)} \cdots \mathbf{P}_X^{(N)}\} \tag{4}$$

with N being the number of atoms in the molecule. Each APT contains the derivatives of the molecular dipole moment with respect to the atomic Cartesian coordinates

$$\mathbf{P}_X^{(\alpha)} = \begin{bmatrix} \frac{\partial p_x}{\partial x_\alpha} & \frac{\partial p_x}{\partial y_\alpha} & \frac{\partial p_x}{\partial z_\alpha} \\ \frac{\partial p_y}{\partial x_\alpha} & \frac{\partial p_y}{\partial y_\alpha} & \frac{\partial p_y}{\partial z_\alpha} \\ \frac{\partial p_z}{\partial x_\alpha} & \frac{\partial p_z}{\partial y_\alpha} & \frac{\partial p_z}{\partial z_\alpha} \end{bmatrix} = \begin{bmatrix} p_{xx}^{(\alpha)} & p_{xy}^{(\alpha)} & p_{xz}^{(\alpha)} \\ p_{yx}^{(\alpha)} & p_{yy}^{(\alpha)} & p_{yz}^{(\alpha)} \\ p_{zx}^{(\alpha)} & p_{zy}^{(\alpha)} & p_{zz}^{(\alpha)} \end{bmatrix} \tag{5}$$

The mean dipole moment derivative of atom α, $\bar{p}_\alpha$, is simply $^1/_3$ of the trace of this matrix[28]

$$\bar{p}_\alpha = 1/3(p_{xx}^{(\alpha)} + p_{yy}^{(\alpha)} + p_{zz}^{(\alpha)}) \tag{6}$$

GAPT charges were calculated from MP2(FC)/6-311++G(3d,3p) wave functions and optimized geometries, whereas the Koopmans' energies were obtained from HF/6-311++G(3d,3p) wave functions using the same geometries as those used to calculate charges. The adiabatic relaxation energies were calculated using HF/6-31G(d,p) wave functions and optimized geometries for both the neutral molecule and the cation. The calculations were carried out on IBM RISC 6000 and DEC Alpha 1000 work stations using the GAMESS[29] and Gaussian 94[30] computer programs.

Results

The potential model, expressed for carbon atom ionization in eq 1 can be written more generally as

$$E_{\alpha,\text{core}} = k_{\alpha,\text{core}} q_\alpha + V + E_{\text{relax}} + E_{0,\alpha} \tag{7}$$

This describes the energy of ionizing an electron in a core orbital of the αth atom in terms of the charge on this atom, q_α, the electrostatic potential owing to the charges of the other atoms in the molecule, V, and the relaxation energy for this ionization

TABLE 1: Experimental 1s Electron Ionization Energies, Koopmans' Energies, Mean Dipole Moment Derivatives, GAPT Charges, and Associated Electrostatic Potentials for Molecules Containing N, O, and B Atoms

molecule	$E_{\alpha,1s}$ (eV)[a]	$E^{Koop}_{\alpha,1s}$(eV)[b]	$\bar{p}_\alpha$ (e)[c]	$V_{\bar{p}\alpha}$ (eV)	q_α (e)[d]	$V_{q\alpha}$ (eV)	E_{relax} (eV)[e]	SE(eV)[f]
				$\alpha = N(sp^3)$				
NH_3	405.57	422.88	−0.101	1.45	−0.436	6.21	−15.83	
NH_2F		426.11			0.050	0.68		
NHF_2		429.48			0.588	−5.44		
NF_3	414.2	432.98	1.15	−12.03	1.157	−12.12	−16.04	
				$\alpha = N(sp)$				
N_2	409.83	426.99	0.000	0.00	0.000	0.00	−14.63	0.00
HCN	406.36	424.64	-0.189	0.99	−0.157	0.44	−16.04	−3.47
ClCN	406.45	424.82	−0.196	2.68	−0.196	2.57	−16.68	−3.38
C_2N_2	407.4	426.25	−0.122	1.73	−0.109	1.53	−16.78	−2.43
BrCN		424.80	−0.192	1.86	−0.187	1.77		
NO	410.85		0.151	−1.89				+1.02
CH_3CN	406.10	423.85	−0.278	1.89	−0.239	1.38	−16.51	−3.73
N*NO	408.66	427.41	−0.281	6.89	−0.275	6.33	−16.23	−1.17
NN*O	412.57	431.43	0.786	−9.73	0.739	−9.07		+2.74
				$\alpha = O$				
O_2	543.81	565.01	0.000	0.00	0.000	0.00	−18.28[g]	0.00
NO	543.54		−0.151	1.89				−0.27
N_2O	541.41	562.40	−0.505	7.81	−0.463	7.31	−19.26	−2.40
F_2CO	540.77	561.27	−0.549	12.33	−0.575	13.00	−19.49	−3.04
OCS	540.3	562.18	−0.581	9.14	−0.588	9.26	−20.81	−3.51
CO_2	541.19	562.09	−0.536	9.99	−0.537	9.93	−19.24	−2.62
CO	542.39	562.44	−0.228	2.91	−0.136	1.72	−18.55	−1.42
H_2CO	539.48	560.00	−0.513	6.50	−0.507	6.44	−19.46	−4.33
Cl_2CO	539.72	561.23	−0.581	11.51	−0.627	12.50	−20.72	−4.09
				$\alpha = B$				
BCl_3	200.15	211.59	0.75	−6.20	1.343	−11.11	−10.49	
BCl_2F		211.80			1.456	−13.69		
$BClF_2$		211.91			1.567	−16.15		
BF_3	202.8	211.96	1.52	−16.78	1.696	−18.58	−7.77	

[a] Experimental values from ref 8. [b] Calculated from HF/6-311++G(3d,3p) wave functions. [c] Experimental values from refs 9−15 and 20. [d] Calculated from MP2(FC)/6-311++G(3d,3p) wave functions. [e] Relaxation energies calculated from ΔSCF method using 6-31G(d,p) wave functions. [f] Substituent effect values. The N_2 and O_2molecules are taken as reference molecules for the N and O atom ionization processes. [g] Calculated from the singlet electronic state.

process. The constants, $k_{\alpha,core}$ and $E_{0,\alpha}$, are determined by regressing energy values on the atomic charges. At the simplest level, E_{relax} is assumed to be zero and experimental ionization energies adjusted by subtracting V are regressed on mean dipole moment derivative values determined from infrared intensities. As such, only experimental data are used to determine the model, and results do not depend on theoretical considerations such as basis set approximations, electron correlation treatment levels, etc. A more complete evaluation of this model adjusts the experimental energies by theoretical relaxation energies because the $k_{\alpha,core}q_\alpha + V$ terms describe a hypothetical ionization process that depends only on the properties of the molecule before it is ionized. As such, $E_{\alpha,core} - V - E_{relax}$ values are regressed on $\bar{p}_\alpha$ values. This calculation involves a mixture of experimental and theoretical results. Finally, the potential model can be evaluated using only theoretical data. Koopmans' energies, as stated earlier, are appropriate to use in simple potential models, and GAPT charges can be used instead of mean dipole moment derivatives. Although the models obtained using theoretical results can suffer from errors in the calculated energies and charges, such as those caused by incomplete basis sets and inadequate electron correlation treatments, they are important to complement experimental data for determining potential models.

Experimental core ionization energies, Koopmans' energies, mean dipole moment derivatives, and GAPT charges are presented in Table 1 for molecules containing B, N, and O atoms. Electrostatic potentials, V, calculated from both the mean dipole moment derivatives and GAPT charges and the relevant internuclear distances obtained from the appropriate experimental[31] or theoretical bond distances and angles are included in this table. For nitrogen containing molecules, different potential models can be anticipated for molecules with $sp^3$and sp hybridized nitrogen atoms. For this reason, the nitrogen data in Table 1 are separated into sp and sp^3 hybridized groups.

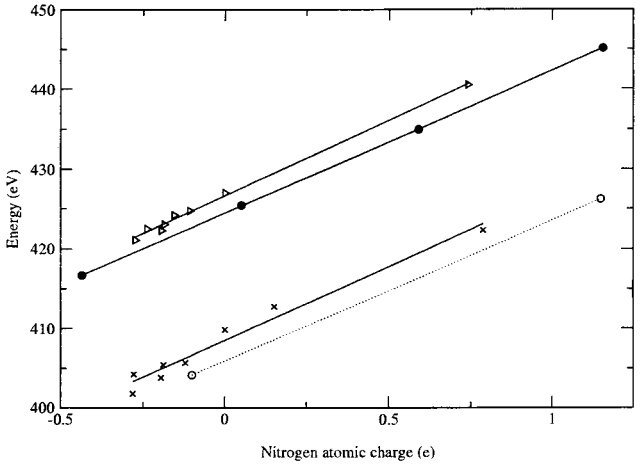

Figure 1. Nitrogen 1s ionization energy adjusted by neighboring atom electrostatic potential vs nitrogen atomic charges: (△) $E^{Koop}_{N,sp,1s} - V$ vs q_N; (●) $E^{Koop}_{N,sp^3,1s} - V$ vs q_N; (×) $E_{N,sp,1s} - V$ vs $\bar{p}_N$; (○) $E_{N,sp^3,1s} - V$ vs $\bar{p}_N$.

Nitrogen. Figure 1 contains Siegbahn potential model plots of experimental ionization energies and mean dipole moment derivatives and of Koopmans' energies and theoretical GAPT charge values for molecules containing sp and sp^3 hybridized

TABLE 2: Regression Statistics for the Simple Potential Models

dependent variable	independent variable	no. of points	slope (V)	intercept (eV)
$E_{N,sp^3,1s} - V$	$\bar{p}_N$	2	17.67	405.91
$E^{Koop}_{N,sp^3,1s} - V$	q_N	4	17.82 (0.05)	424.47 (0.03)
$E_{N,sp^3,1s} - V - E_{relax}$	$\bar{p}_N$	2	17.84	421.75
$E_{N,sp,1s} - V$	$\bar{p}_N$	8	18.55 (1.31)	408.51 (0.44)
$E^{Koop}_{N,sp,1s} - V$	q_N	8	18.90 (0.50)	426.65 (0.16)
$E_{N,sp,1s} - V - E_{relax}$	$\bar{p}_N$	6	18.60 (4.20)	424.55 (0.85)
$E_{O,1s} - V$	$\bar{p}_O$	9	25.49 (2.47)	544.82 (1.12)
$E^{Koop}_{O,1s} - V$	q_O	8	23.87 (2.75)	564.80 (1.32)
$E_{O,1s} - V - E_{relax}$	$\bar{p}_O$	7	23.50 (5.78)	563.53 (2.96)
$E_{F,1s} - V$	$\bar{p}_F$	19	22.67 (1.71)	696.55 (0.83)
$E^{Koop}_{F,1s} - V$	q_F	19	19.14 (1.78)	718.08 (0.98)
$E_{B,1s} - V$	$\bar{p}_B$	2	17.18	193.46
$E^{Koop}_{B,1s} - V$	q_B	4	22.26 (0.92)	192.97 (1.40)
$E_{P,1s} - V$	$\bar{p}_P$	2	12.89	2149.71
$E^{Koop}_{P,1s} - V$	q_P	4	12.38 (0.06)	2174.59 (0.08)
$E^{Koop}_{P,2s} - V$	q_P	4	12.01 (0.07)	203.07 (0.08)
$E_{P,2p} - V$	$\bar{p}_P$	2	12.34	136.40
$E^{Koop}_{P,2p} - V$	q_P	4	11.99 (0.07)	145.76 (0.09)
$E^{Koop}_{Cl,1s} - V$	q_{Cl}	17	13.00 (1.15)	2853.35 (0.44)
$E_{Cl,2s} - V$	$\bar{p}_{Cl}$	9	15.55 (5.12)	277.84 (1.18)
$E^{Koop}_{Cl,2s} - V$	q_{Cl}	17	12.85 (1.12)	287.98 (0.43)
$E_{Cl,2p} - V$	$\bar{p}_{Cl}$	12	15.91 (4.26)	207.08 (1.02)
$E^{Koop}_{Cl,2p} - V$	q_{Cl}	17	12.82 (1.12)	219.02 (0.43)
$E^{Koop}_{Br,1s} - V$	q_{Br}	6	11.36 (0.16)	13335.87 (0.08)
$E^{Koop}_{Br,2s} - V$	q_{Br}	6	11.31 (0.17)	1774.57 (0.08)
$E^{Koop}_{Br,2p} - V$	q_{Br}	6	11.30 (0.17)	1593.87 (0.08)
$E^{Koop}_{Br,3s} - V$	q_{Br}	6	11.29 (0.17)	269.01 (0.08)
$E^{Koop}_{Br,3p} - V$	q_{Br}	6	11.25 (0.17)	203.91 (0.08)
$E^{Koop}_{Br,3d} - V$	q_{Br}	6	11.27 (0.17)	87.95 (0.08)

nitrogen atoms. In both cases, the appropriate neighboring atom electrostatic potential is subtracted from the energy.

Both 1s electron ionization energies and gas-phase fundamental infrared intensities have been measured for eight molecules containing sp hybridized nitrogens. The graphs in Figure 1 show that the simple potential model is obeyed by both the experimental and theoretical data. The coefficient of determination, R^2, is higher for the theoretical $E^{Koop}_{N,sp,1s} - V$ vs q_N regression (0.9959) than for the $E_{N,sp,1s} - V$ vs $\bar{p}_N$ regression (0.9708) because the experimental energies include contributions from the relaxation process that are not considered in the simple potential model.

The vertical displacements of the lines are expected because relaxation energies have often been assumed to be similar for groups of similar molecules.[32] As the quality of the quantum chemical wave functions improves, the simple potential models for the experimental data containing adjustments for the relaxation effects become more similar to the potential models obtained with Koopmans' energies. This occurs for the nitrogen containing molecules treated here, and a detailed study of this effect has been reported for the potential models involving sp^3, sp^2, and sp carbon atoms.[4] Although a graph of $E_{N,sp,1s} - V - E_{relax}$ vs $\bar{p}_N$ has not been included in Figure 1, the regression statistics for its potential model have been included in Table 2. Although the slope value increases only slightly, the intercept increases by 16 eV when relaxation energy adjustments to the experimental ionization energies are made. These values are close to the ones obtained for the potential model with Koopmans' energies as expected.

Experimental 1s electron ionization energies and mean dipole moment derivatives have only been measured for NH_3 and NF_3 for the sp^3 nitrogen atom containing molecules. This is not sufficient to test the validity of the simple potential model for this hybridization state of nitrogen. For this reason, Koopmans' energies and GAPT charges were calculated for NH_3, NH_2F, NHF_2, and NF_3. Note that the graph of the $E^{Koop}_{N,sp^3,1s} - V$ energies against the GAPT charges in Figure 1 results in a straight line with the regression statistics given in Table 2. This seems to warrant assuming a linear potential model for the NH_3 and NF_3 experimental data. It is reassuring that both models have very similar slopes. As expected, the potential model graph of $E_{N,sp^3,1s} - V - E_{relax}$ vs $\bar{p}_N$ approximates the $E^{Koop}_{N,sp^3,1s} - V$ vs q_N line as can be seen from the regression statistic results in Table 2.

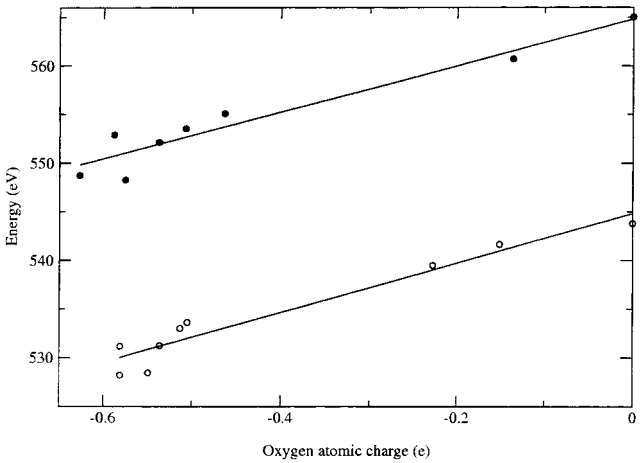

Figure 2. Oxygen 1s ionization energy adjusted by neighboring atom electrostatic potential vs oxygen atomic charges: (●) $E^{Koop}_{O,1s} - V$ vs q_O; (○) $E_{O,1s} - V$ vs $\bar{p}_O$.

Oxygen. Figure 2 contains a graph of oxygen atom 1s electron ionization energies as a function of atomic charge. The lower regression line represents the model for points completely determined from experimental X-ray ionization, vibrational

TABLE 3: Experimental 1s Electron Ionization Energies, Koopmans' Energies, Mean Dipole Moment Derivatives, GAPT Charges, and Associated Electrostatic Potentials for Molecules Containing F Atoms

molecule	$E_{F,1s}$ (eV)[a]	$E_{F,1s}^{Koop}$ (eV)[b]	$\bar{p}_F$ (*e*)[c]	$V\bar{p}_F$ (eV)	q_F (e)[d]	V_{qF} (eV)	SE (eV)[e]
F_2	696.69	719.34	0.000	0.00	0.000	0.00	0.00
SiF_4	694.70	716.89	−0.554	11.10	−0.602	11.89	−1.99
PF_3	694.15	716.91	−0.58	8.90	−0.604	9.13	−2.54
NF_3	694.45	718.25	−0.38	6.99	−0.386	6.92	−2.24
NaF		709.36	−0.889	6.65	−0.920	6.69	
LiF		710.58	−0.861	7.93	−0.859	7.76	
HF	694.18	715.65	−0.382	6.00	−0.389	6.10	−2.51
F_2CS		718.05	−0.453	8.15	−0.554	9.58	
F_2CO	695.43	718.21	−0.483	9.73	−0.516	10.30	−1.26
CF_4	695.48	717.82	−0.512	12.06	−0.510	12.00	−1.21
CHF_3	694.36	716.97	−0.506	9.77	−0.524	10.00	−2.33
CH_2F_2	693.65	716.05	−0.488	7.31	−0.522	7.78	−3.04
CH_3F	692.66	715.05	−0.490	5.27	−0.501	5.33	−4.03
CF_3Cl	695.04	717.65	−0.590	12.04	−0.539	11.57	−1.65
CF_2Cl_2	694.68	717.50	−0.577	11.03	−0.553	11.05	−2.01
$CFCl_3$	694.33	717.36	−0.478	9.40	−0.556	10.37	−2.36
C_6F_6	694.20		−0.410	6.34			−2.49
C_2F_6	695.07	717.86	−0.443	10.17			−1.62
BF_3	694.8	716.86	−0.510	10.21	−0.565	11.43	−1.89
CH_2CF_2	694.44	717.03	−0.423	6.91	−0.503	8.03	−2.25
FCl	694.36	717.31			−0.274	2.38	−2.23
CF_3I	694.63		−0.582	11.35			−2.06
CF_3Br	694.75		−0.542	11.09			−1.94

[a] Experimental values from ref 8. [b] Calculated from HF/6-311++G(3d,3p) wave functions. [c] Experimental values from refs 3, 8, 9, 11, 13, 14, 17, and 21−23. [d] Calculated from MP2(FC)/6-311++G(3d,3p) wave functions. [e] Substituent effect values. The F_2 molecule is taken as the reference molecule for the F atom ionization processes.

frequency, and infrared intensity data. The upper regression line corresponds to a model using Koopmans' energies and theoretical GAPT charges. Regression statistics for all models are given in Table 2. A regression line for the $E_{O,1s} - V - E_{relax}$ vs $\bar{p}_O$ has not been included in Figure 2. Note, however, that the inclusion of the relaxation energy adjustments to the experimental ionization energies results in slope and intercept values in close agreement with the $E_{O,1s}^{Koop} - V$ vs q_O values and much different from those found for the experimental ionization energies. The oxygen models are more difficult to evaluate than the nitrogen ones because the mean dipole moment derivatives for the oxygen molecules studied span a range of only 0.6 *e*, whereas the nitrogen values vary by about 1.5 *e*. Furthermore, most of the oxygen containing molecules for which appropriate experimental data exist have values between 0.5 and 0.6 *e*. For this reason, the data for the molecules with values outside this interval (O_2, 0.0 *e*; NO, −0.151 *e*; and CO, −0.228 *e*) exert high leverages on the regressions and have a strong influence in determining the model parameter values. The slopes range from 23.5 to 25.5 V, substantially larger than those found for the nitrogen models. This ordering is consistent with the one expected from potential model considerations because the covalent radius of the oxygen atom is smaller than the nitrogen one.

Fluorine. Most of the fluorine containing molecules for which appropriate experimental data exist have experimental mean dipole moment derivatives between −0.4 and −0.6 *e*. For this reason, the fluorine molecule, $q_F = 0$ *e* and $\bar{p}_F = 0$ *e*, and the NaF and LiF molecules with $q_F = -0.920$ and −0.859 *e*, respectively, are particularly influential in determining model parameters. The potential model graphs obtained using the data for the fluorine atoms in Table 3 are shown in Figure 3. The regression statistics have been included in Table 2. The coefficients of determination are close to 0.95 for these models. Their slopes have values that are about 3−4 V smaller than the values obtained for the corresponding oxygen atom models. However, this ordering is in agreement with the simple model prediction that the slopes vary proportionally with the inverse

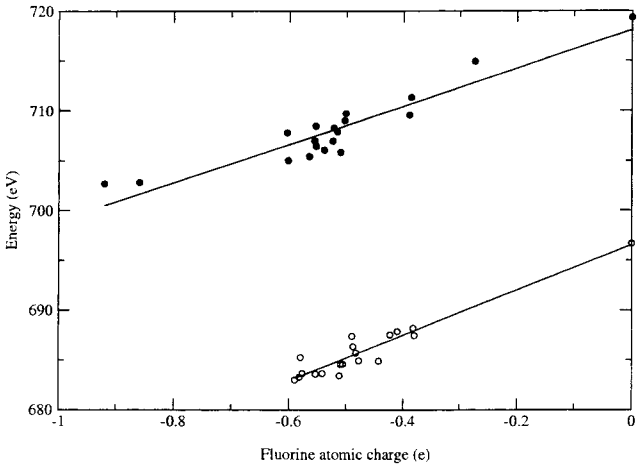

Figure 3. Fluorine 1s ionization energy adjusted by neighboring atom electrostatic potential vs fluorine atomic charges: (●) $E_{F,1s}^{Koop} - V$ vs q_F; (○) $E_{F,1s} - V$ vs $\bar{p}_F$.

covalent radii of these atoms. It must be remembered that the oxygen atoms with double bonds present smaller covalent radii than those of fluorines with single bonds.

As mentioned earlier, experimental data to evaluate the potential models for the 1s ionization processes for the boron and phosphorus atoms are quite limited. For this reason ab initio theoretical data are important to supplement the experimental data. Although the data strongly suggest that simple potential models are valid for both atoms, there are large discrepancies between the experimental and theoretical results for the boron atom.

Boron. The boron potential model plots corresponding to the data in Table 1, and the regression statistics in Table 2 for the boron containing molecules are shown in Figure 4. Contrary to the situation for the phosphorus containing molecules, as will be seen, the experimental and theoretical results are not in good agreement. Although the boron mean dipole moment derivative, 1.52 *e*, is in reasonable agreement with the theoretical GAPT

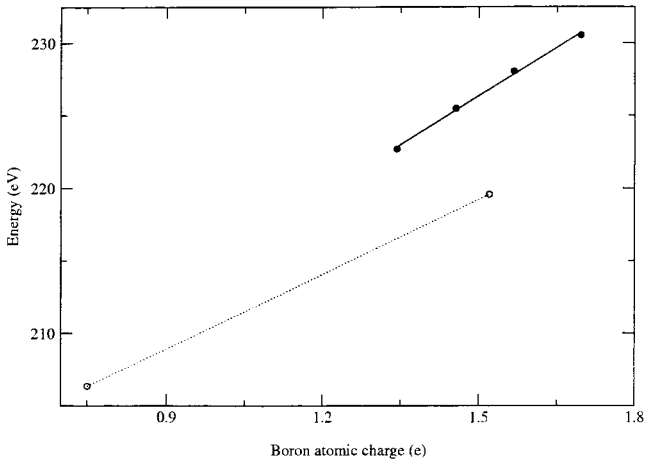

Figure 4. Boron 1s ionization energy adjusted by neighboring atom electrostatic potential vs boron atomic charges: (●) $E^{\text{Koop}}_{\text{B,1s}} - V$ vs q_{B}; (○) $E_{\text{B,1s}} - V$ vs $\bar{p}_{\text{B}}$.

TABLE 4: HF/6-311++G(3d,3p) Koopmans' Energies for 1s, 2s, and 2p Electrons, MP2(FC)/6-311++G(3d,3p) GAPT Charges, Experimental 1s, 2s, and 2p Electron Ionization Energies, and Mean Dipole Moment Derivatives for Phosphorus Atom of the PH_xF_{3-x} $x = 0$, 1, 2, and 3 Series

experiment	$E_{\text{P,1s}}$ (eV)[a]	$E_{\text{P,2s}}$ (eV)[a]	$E_{\text{P,2p}}$ (eV)[a]	$\bar{p}_{\text{P}}$ (e)[b]	V $\bar{p}_{\text{P}}$ (eV)
PH_3	2150.69		137.19	0.357	−3.62
PF_3	2156.18	199.6	141.92	1.74	−15.96
theory	$E^{\text{Koop}}_{\text{P,1s}}$ (eV)	$E^{\text{Koop}}_{\text{P,2s}}$ (eV)	$E^{\text{Koop}}_{\text{P,2p}}$ (eV)	q_{P} (e)	$V_{q\text{P}}$ (eV)
PH_3	2175.30	203.67	146.35	0.310	−3.17
PH_2F	2177.18	205.35	148.02	0.838	−7.75
PHF_2	2178.96	206.94	149.60	1.348	−12.25
PF_3	2180.68	208.49	151.15	1.813	−16.41

[a] Experimental values from ref 8. [b] Experimental values from ref 10.

charge of 1.70 e for BF_3, the value for the B mean derivative in BCl_3 is about 0.6 e smaller than the B GAPT charge. As such, the lack of agreement between the mean dipole moment derivatives and the GAPT charges, specially for the boron atom of BCl_3, is the major factor provoking the difference between the theoretical and experimental models shown in Figure 4. In any case, the $E^{\text{Koop}}_{\text{B,1s}} - V$ vs q_{B} theoretical plot strongly suggests that the potential model is indeed linear for the boron atom. The points for BF_3, BF_2Cl, $BFCl_2$, and BCl_3 fall nicely on a straight line. An assumed linear model for the experimental points results in a model with a slope 5 V lower than the theoretical one. However, the intercepts are almost the same, 193.46 and 192.97 eV.

Phosphorus. Experimental 1s and 2p electron ionization energies for the phosphorus atoms in PH_3 and PF_3 are presented in Table 4 along with their mean dipole moment derivatives. Unfortunately analogous experimental results are not known for PH_2F and PHF_2, and the 2s ionization energy for PH_3 has not been reported in the literature to our knowledge. Complementing these experimental results theoretical Koopmans' energy and GAPT charge values are included in this table. The theoretical and experimental phosphorus mean dipole moment derivatives agree within 0.05 and 0.07 e respectively for PH_3 and PF_3. Potential model graphs for the phosphorus 1s, 2s, and 2p electrons are presented in Figure 5 for the theoretical values of the PH_xF_{3-x} $x = 0$, 1, 2, 3 series as well as for the experimental 1s and 2p electron ionization and mean dipole moment derivative values. As seen for the analogous nitrogen compounds, the $E^{\text{Koop}}_{\text{P,core}} - V$ vs q_{P} plots result in very straight lines. The slopes of these lines are close to being parallel to the potential model lines assumed to join the PH_3 and PF_3 experimental data points in Figure 5. It can be seen there that linear potential models are predicted for 1s, 2s, and 2p theoretical Koopmans' energies. The slopes of the regression lines are approximately equal, 12.38, 12.01, and 11.99 V, suggesting that substituent effects on the 1s, 2s, and 2p ionization energies are about the same. Approximately equal slopes, 12.89 and 12.34 V for the 1s and 2p electron potential models, are also observed for the experimental ionization energies and mean dipole moment derivatives. This is simply another way of saying what has been known for some time: different core levels on the same atom shift by approximately the same amount when going from one molecule to another. This is also consistent with eq 7 if the $k_{\alpha,\text{core}}$ is the same for 1s, 2s, and 2p electrons and relaxation energies for 1s, 2s, and 2p electron ionization processes suffer similar substituent shifts. Classical electrostatic considerations show that $k_{\alpha,\text{core}}$ values are inversely proportional to the average difference of the distance between the valence electron and core electron. Theoretical considerations show that these distances are almost the same, so nearly constant $k_{\alpha,\text{core}}$ values are expected.

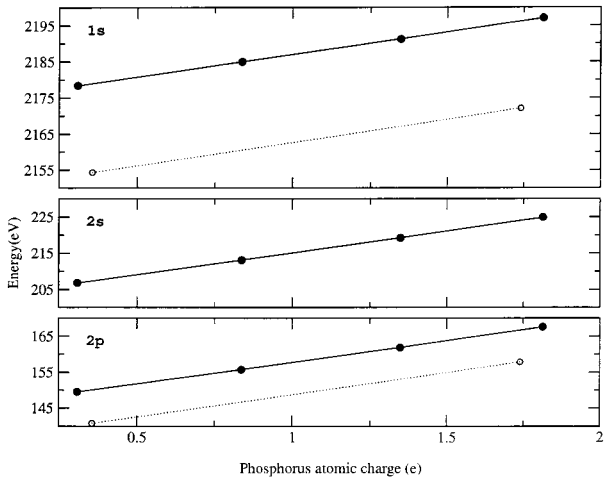

Figure 5. Phosphorus 1s, 2s, and 2p Koopmans' energies and experimental 1s and 2p phosphorus ionization energies adjusted by neighboring atom electrostatic potentials vs phosphorus GAPT charges and mean dipole moment derivatives, respectively: (●) $E^{\text{Koop}}_{\text{P,core}} - V$ vs q_{P}; (○) $E_{\text{P,core}} - V$ vs $\bar{p}_{\text{P}}$.

Chlorine. Behavior of the core ionization energies of chlorine are especially interesting applications of the potential model because experimental energies are available for the ionization of both the 2s and 2p electrons in several molecules. If the average electrostatic interactions of the 2s and 2p electrons with the valence electrons are about the same, one can expect potential model $E-V$ plots with close to identical slopes. Under this condition the $k_\alpha \bar{p}_\alpha$ and V terms do not depend on which of the core electrons is ionized. As such, the potential model predicts that the differences between the 2s and 2p ionization energies, $E_{\text{Cl,2s}} - E_{\text{Cl,2p}}$, do not depend on the molecular environment, similar to the behavior observed for the phosphorus 1s and 2p electrons. This conclusion can be tested using the data in Table 5 where both 2s and 2p experimental ionization energies are given for nine molecules. The differences, not given in this table, are remarkably constant 70.99 ± 0.07 eV. This standard deviation is well within the expected experimental error of 0.1 eV. Constant differences are also found for the Koopmans' energies presented in the bottom part of Table 5. The 1s−2s difference is 2565.34 ± 0.06 eV, the 2s−2p difference,

TABLE 5: Experimental 2s and 2p Electron Ionization Energies, Mean Dipole Moment Derivatives, and Substituent Effects and Their Analogous Theoretical Quantities, HF/6-311++G(3d,3p) Koopmans' Energies for 1s, 2s, and 2p Electrons, MP2(FC)/6-311++G(3d,3p) GAPT Charges, and Substituent Effects for Molecules Containing Cl Atoms

experimental	$E_{Cl,1s}$ (eV)	$E_{Cl,2s}$ (eV)[a]	$E_{Cl,2p}$ (eV)[a]	$\bar{p}_{Cl}$ (e)[b]	$V\bar{p}_{Cl}$ (eV)	1s SE (eV)[c]	2s SE (eV)[c]	2p SE (eV)[c]
Cl_2		278.74	207.82	0.000	0.00		0.00	0.00
HCl			207.38	−0.183	2.07			−0.44
cis-$C_2H_2Cl_2$		277.77	206.82	−0.203	1.78		−0.97	−1.00
CH_3Cl		277.2	206.25	−0.271	2.20		−1.54	−1.57
CH_2Cl_2		277.6	206.66	−0.248	2.90		−1.14	−1.16
$CHCl_3$		277.75	206.83	−0.267	3.99		−0.94	−0.99
CCl_4		278.02	207.02	−0.261	4.59		−0.72	−0.80
CF_3Cl		278.84	207.83	−0.139	5.63		+0.10	+0.01
CF_2Cl_2		278.63	207.47	−0.236	5.50		−0.11	−0.35
$CFCl_3$		278.24	207.20	−0.297	5.56		−0.50	−0.62
Cl_2CO		−	207.40	−0.331	5.40			−0.42
BCl_3		−	207.0	−0.250	3.81			−0.82
theoretical	$E^{Koop}_{Cl,1s}$ (eV)	$E^{Koop}_{Cl,2s}$ (eV)	$E^{Koop}_{Cl,2p}$ (eV)	q_{Cl} (e)	V_{qCl} (eV)	1s SE (eV)[c]	2s SE (eV)[c]	2p SE (eV)[c]
Cl_2	2854.50	289.07	220.10	0.000	0.00	0.00	0.00	0.00
NaCl	2849.11	283.78	214.85	−0.829	4.96	−5.39	−5.29	−5.25
LiCl	2849.80	284.49	215.56	−0.787	5.54	−4.70	−4.58	−4.54
HCl	2853.06	287.75	218.81	−0.195	2.21	−1.44	−1.32	−1.29
ClCN	2855.39	290.04	221.09	−0.023	0.93	+0.89	+0.97	+0.99
cis-$C_2H_2Cl_2$	2853.19	287.87	218.93	−0.218	1.85	−1.31	−1.20	−1.17
CH_3Cl	2852.40	287.07	218.13	−0.275	2.23	−2.10	−2.00	−1.97
CH_2Cl_2	2853.05	287.73	218.78	−0.284	3.27	−1.45	−1.34	−1.32
$CHCl_3$	2853.51	288.19	219.24	−0.289	4.28	−0.99	−0.88	−0.86
CCl_4	2853.82	288.51	219.56	−0.298	5.27	−0.68	−0.56	−0.54
CF_3Cl	2854.08	288.78	219.83	−0.246	6.19	−0.42	−0.29	−0.27
CF_2Cl_2	2853.97	288.67	219.72	−0.281	6.02	−0.53	−0.40	−0.38
$CFCl_3$	2853.89	288.58	219.63	−0.296	5.71	−0.61	−0.49	−0.47
Cl_2CO	2854.17	288.85	219.90	−0.368	5.96	−0.33	−0.22	−0.20
BCl_3	2853.39	288.12	219.18	−0.448	6.83	−1.40	−0.95	−0.90
Cl_2CS	2854.06	288.74	219.79	−0.373	5.25	−0.44	−0.33	−0.31
FCl	2855.57	290.05	221.08	0.274	−2.38	+1.07	+0.98	+0.98

[a] Experimental values from ref 8. [b] Experimental values from refs 8, 9, 14, 17−19. [c] Substituent effect values. The Cl_2 molecule is the reference molecule for the Cl atom ionization processes.

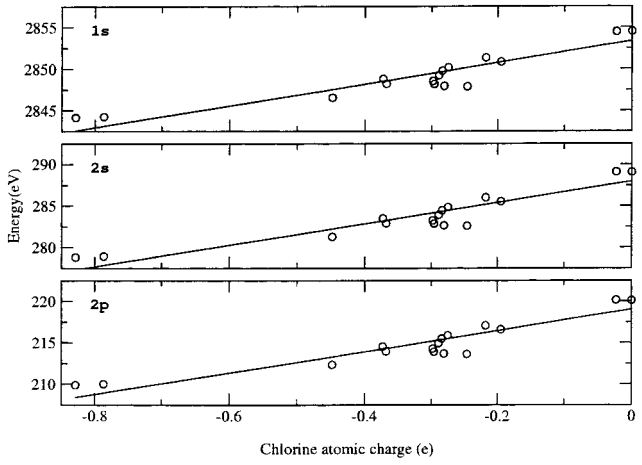

Figure 6. Chlorine 1s, 2s, and 2p Koopmans' energies adjusted by neighboring atom electrostatic potential vs chlorine GAPT charges.

68.95 ± 0.01 eV, and the 1s−2p difference, 2634.29 ± 0.07 eV.

In Figure 6, potential model graphs are shown for the 1s, 2s, and 2p HF/6-311++G(3d,3p) Koopmans' energies and the MP2(FC)/6-311++G(3d,3p) GAPT charges. Regression correlation coefficients of about 0.95 are obtained for all three potential models that have very similar slopes, 13.00, 12.85, and 12.82 V, as can be seen in Table 2. Models for the experimental 2s and 2p ionization energies and mean dipole moment derivatives are not shown. Although the linear tendencies are clearly present, scatters of points about the regression lines are substantially larger and regression correlation coefficients are smaller, around 0.75, for the models obtained with experimental data.

Table 5 includes values of the substituent effects on the Cl atom 1s, 2s, and 2p ionization energies owing to substitution of one of the chlorines in Cl_2 by another atom or group of atoms. Similar to results observed for the phosphorus 1s and 2p electron ionization energies, the substituent effects on the chlorine 2s and 2p experimental ionization energies are seen to be almost the same with an average difference of 0.08 eV. Although this value is smaller than the experimental error in measuring a core electron ionization energy (about 0.1 eV), the differences in the experimental 2s and 2p values are hardly attributable to random experimental errors because all of the 2p substituent effect values are more negative than the 2s ones. Because theoretical considerations indicate that the average 2s valence electron distances are slightly larger than the 2p valence ones, the 2p electron potential model plots can be expected to have slightly larger slope values and hence slightly larger absolute values for substituent effects. On the other hand, the Koopmans' energy results show the opposite trend. The 1s Koopmans' energies are, on the average, 0.13 eV smaller than the 2s energies, which are, in turn, 0.03 eV smaller than the 2p ones.

Bromine. Table 6 contains HF/6-311++G(3d,3p) Koopmans' energies for the 1s, 2s, 2p, 3s, 3p, and 3d electrons for the bromine atom in Br_2, BrCN, NaBr, LiBr, FBr, and ClBr along with the Br atom GAPT charges. The bottom part of the table contains the substituent effects, $E^{Koop}_{Br,nl}(XBr) - E^{Koop}_{Br,nl}(Br_2)$. Note that the substituent effect values are almost the same (within 0.1 eV) for the molecules in the table. No clear trends in substituent effect values can be observed as the ionized electron is taken from core orbitals with increasing principal

TABLE 6: HF/6-311++G(3d,3p) Koopmans' Energies for 1s, 2s, 2p, 3s, 3p, and 3d Electrons, MP2(FC)/6-311++G(3d,3p) GAPT Charges, and Substituent Effects for Molecules Containing Br Atoms

Theoretical

molecule	$E^{Koop}_{Br,1s}$ (eV)	$E^{Koop}_{Br,2s}$ (eV)	$E^{Koop}_{Br,2p}$ (eV)	$E^{Koop}_{Br,3s}$ (eV)	$E^{Koop}_{Br,3p}$ (eV)	$E^{Koop}_{Br,3d}$ (eV)	q_{Br} (e)	V_{qBr} (eV)
Br_2	13335.87	1774.58	1593.88	269.02	203.92	87.96	0.000	0.00
BrCN	13336.88	1775.60	1594.90	270.05	204.96	88.99	0.070	0.03
NaBr	13331.42	1770.17	1589.48	264.61	199.55	83.57	−0.805	4.54
LiBr	13332.03	1770.78	1590.08	265.23	200.16	84.18	−0.758	4.96
FBr	13336.98	1775.65	1594.95	270.06	204.95	88.99	0.338	−2.72
ClBr	13336.16	1774.87	1594.17	269.30	204.20	88.24	0.099	−0.66

Substituent Effect[a]

molecule	1s SE (eV)	2s SE (eV)	2p SE (eV)	3s SE (eV)	3p SE (eV)	3d SE (eV)	average (eV)	SD (eV)
Br_2	0.00	0.00	0.00	0.00	0.00	0.00	0.00	0.000
BrCN	1.01	1.02	1.02	1.03	1.04	1.03	1.023	0.011
NaBr	−4.45	−4.41	−4.40	−4.41	−4.37	−4.39	−4.405	0.027
LiBr	−3.84	−3.80	−3.80	−3.79	−3.76	−3.78	−3.792	0.027
FBr	1.11	1.07	1.07	1.04	1.03	1.03	1.058	0.031
ClBr	0.29	0.29	0.29	0.28	0.28	0.28	0.285	0.005

[a] Substituent effect values using Br_2 as a reference molecule for the Br atom ionization processes.

and azimuthal quantum numbers, n and l. Although substituent effect values decrease for FBr as n changes from one to three, an opposite effect occurs for BrCN where the $n = 3$ substituent effect values are slightly larger (0.01−0.03 eV) than the value for the 1s orbital.

Discussion

Simple potential models do not compete in accuracy with high quality quantum chemical results,[33,34] but they are useful in explaining ionization energy variations in terms of point charges of atoms in molecules. The mean dipole moment derivatives, obtained from the experimental intensities, or the GAPT charges, calculated from molecular wave functions provide the values for the point charges.

All of the oxygen substituent effect values in Table 1 are negative. Compared to the O_2 molecule where an oxygen atom substituent is bound to the oxygen atom being ionized, the other oxygen containing molecules in the table have less electronegative substituents. This results in negative oxygen partial charges on the oxygen atom being ionized that is confirmed by the negative mean dipole moment derivative and GAPT charge values for the ionizing oxygen atoms. Now the substituent effect

$$E_{XO} - E_{O_2} = k(q_O)_{XO} + V_{XO} \qquad (8)$$

is negative having a predominant negative contribution from the first term on the right because $(q_O)_{XO}$ is negative.

For the sp nitrogen containing molecules in Table 1, all substituent effects are negative except those for NO and NN*O. The substituents bound to the ionizing nitrogen atoms in all of the molecules but these two have average electronegativities that are smaller than the nitrogen atom electronegativity. Again this is confirmed by the signs of the sp nitrogen atom mean dipole moment derivative and GAPT charge values in Table 1. The $k_N q_N$ terms provide larger contributions to the substituent effects than those from the electrostatic potentials of the neighboring atoms.

By this same line of reasoning, the 1s electron ionization energy for NF_3 is larger than the one for NH_3. In fact, the GAPT charges and mean dipole moment derivatives of nitrogen are positive for NF_3 and negative for ammonia. The 1s ionization energy of BF_3 is higher than the one for BCl_3 as expected. It is more difficult to ionize a core electron from a boron atom with a +1.52 e charge (or +1.70 e for the theoretical charge) than from one with a +0.75 e charge (or +1.34 e theoretical value).

In Table 3, all of the substituent effects on the 1s F electron ionization are negative as expected. Because fluorine is the most electronegative atom, any possible substituent will have an average electronegativity value less than the fluorine one. Again, the kq terms dominate the V ones.

The PF_3 1s and 2p phosphorus electron experimental ionization energies are each larger than their analogous energies for PH_3. The phosphorus charge in PF_3 is +1.74 e (or +1.81 e from molecular orbital calculations), much more positive than it is in PH_3, +0.36 e (or +0.31 e theoretical value).

The substituent effects on the chlorine atom calculated from experimental ionization energies are all negative except for the CF_3Cl one as can be observed in Table 5. Both of the CF_3Cl substituent effects on the 2s and 2p chlorine electron ionization energies are slightly positive. However, this is not because the chlorine atom being ionized is positively charged. Indeed its mean dipole moment derivative is negative, −0.139 e. However, the V term in eq 8 also provides an important contribution because the carbon atom neighboring the chlorine atom is very positive (mean dipole moment derivative of +1.5 e) owing to the three electronegative fluorines bound to it. This positive contribution to the substituent effect is slightly larger than the negative one from the $k_{Cl}\,\bar{p}_{Cl}$ term. For the substituent effects calculated from the Koopmans' energies in Table 5, only ClCN and FCl are positive. The chlorine GAPT charge is quite positive in FCl, indicating $k_{Cl}q_{Cl}$ predominance, whereas it is almost zero but slightly negative in ClCN. The V term provides an important contribution for ClCN because the carbon atom bound to the Cl one is very positively charged owing to electron density lost to its nitrogen neighbor. The CF_3Cl substituent effects obtained from the Koopmans' energies are of opposite sign to those calculated from the experimental values. The calculated chlorine GAPT charge, −0.246 e, is about 0.1 e more negative than the one obtained from the experimental intensities accounting for the differences.

The substituent effects on the 1s, 2s, 2p, 3s, 3p, and 3d Br atom electron ionization energies are analogous to those found for chlorine electron ionization. The FBr and BrCN molecules exhibit quite positive substituent effects because the F and CN substituents are more electronegative than the Br atom. On the other hand, the NaBr and LiBr substituent effects are very negative because Na and Li are less electronegative than Br.

TABLE 7: Theoretical Values of ⟨1s1s|*nsns*⟩ Coulomb Integrals and Inverses of Average Distances and Experimental Slope Values from Potential Models and Inverse Standard Covalent Radii (Atomic Units)

⟨1s1s | 2s2s⟩	Coulomb integrals[a]	$1/\langle r\rangle^a$	k^b	$1/r_{cov}{}^c$
B	0.646	0.520	0.631 ± 0.034^d	0.654
C	0.808	0.650	0.658 ± 0.033^e	0.777^e
N	0.895	0.780	0.666 ± 0.048^e	0.820^e
O	1.130	0.910	0.937 ± 0.091	0.855
F	1.291	1.040	0.833 ± 0.063	0.735
⟨1s1s|3s3s⟩	Coulomb integrals[a]	$1/\langle r\rangle^a$	k^b	$1/r_{cov}{}^c$
Si	0.461	0.395	0.453 ± 0.007^d	0.452
P	0.533	0.457	0.474 ± 0.002^d	0.481
Cl	0.678	0.581	0.578 ± 0.172	0.535
⟨1s1s|4s4s⟩	Coulomb integrals[a]	$1/\langle r\rangle^a$	k^b	$1/r_{cov}{}^c$
Ge	0.382	0.339	0.405 ± 0.010^f	0.433
Br	0.514	0.456	0.415 ± 0.006^f	0.465

[a] Calculated using Slater orbitals having standard exponential coefficients. [b] Slopes from experimental $E_{\alpha,core} - V$ vs $\bar{p}_\alpha$ plots. [c] Values taken from Reference 35. [d] Standard deviation values obtained from potential models using Koopmans' energies and GAPT charges. [e] Average values for the different hybridization states studied here. [f] Values obtained from potential models using Koopmans' energies and GAPT charges.

The ClBr molecule shows positive substituent effects as expected because Cl is more electronegative than Br. However, their values are close to 1 eV smaller than those for BrCN and FBr.

The slope values of potential models are interpreted as representing electrostatic interactions between core and valence electrons. These interactions can be calculated from coulomb integrals, $\langle\phi_c{}^2(1)|r_{12}{}^{-1}|\phi_v{}^2(2)\rangle$, involving core and valence orbitals, ϕ_c and ϕ_v, respectively. Table 7 contains coulomb integral values calculated using Slater orbitals with standard exponents for B, C, N, O, F, Si, P, Cl, Ge, and Br atoms. These values can be compared with the slope values of simple potential models that are given in the third column of this table. Most of these slope values are taken from Table 2 except for the sp, sp^2, and sp^3carbon and sp^3 Si and Ge slopes that were taken from our earlier publications.[3−5] Except for the Ge and Br values that correspond to potential models based on theoretical results, all other values in this column are from models using only experimental data. There is considerable agreement between the coulomb integral and slope values in Table 7 if we take into account that atomic Slater orbitals are only rough approximations to orbitals in molecules. Furthermore some of the experimental slope values have rather large experimental uncertainties.

These coulomb integral values can be expected to vary proportionally with the inverse covalent radii of the valence orbitals because the core orbitals are so close to the nuclei. Inverses of average distances calculated for the Slater valence orbitals are given in the second column of Table 7. Figure 7 shows a graph of the coulomb integral values against the inverse of the average Slater valence orbital radii. These theoretical points, represented by darkened circles, fall on a straight line confirming the inverse proportionality between coulomb integrals and average distances of the valence electrons from the nuclei, approximating the average core−valence electron separations. The open circles in the graph of Figure 7 correspond to the potential model slope values from Table 2 and to

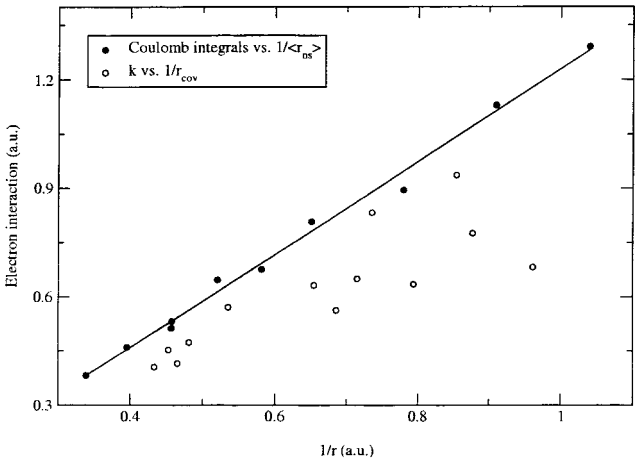

Figure 7. Coulomb integrals and potential model slopes graphed against inverse average and covalent radii.

corresponding standard covalent radii taken from Pauling's classic book.[35] All of the open circles have coordinates obtained from only experimental data except for the Ge and Br ones for which experimental data are not sufficient to estimate potential models. The O, F, B, P, Cl, Si, Ge, and Br points exhibit quite linear behavior and fall slightly below the theoretical line. This indicates that core−valence electron repulsions for these atoms are smaller in molecules than might be expected in the isolated atoms. This effect is larger for the sp, sp^2, and sp^3 carbon atoms and the sp and sp^3 nitrogen ones as can be seen in Figure 7.

The theoretical linear model in Figure 7 can be expressed by the regression equation

$$k \cong \langle\phi_c{}^2(1)|r_{12}{}^{-1}|\phi_v{}^2(2)\rangle = 1.28\left(\frac{1}{\langle r\rangle}\right) + 0.02 \qquad (9)$$

Indeed, the intercept is expected to be zero because the coulomb integral value vanishes as $\langle r\rangle$, the average Slater orbital radius, goes to infinity. The 1.28 slope value is close to the value expected for spherically uniform charge distributions. The energy necessary to build up such a distribution with total charge, q, is

$$E = \frac{3}{5}\frac{q^2}{r} \qquad (10)$$

where r is the radius of the sphere.[36]

The difference in energy for such distributions with $q + 1$ and q total charges is

$$\Delta E = \frac{6}{5r}\left(q + \frac{1}{2}\right) \qquad (11)$$

The slope of 1.28 can be compared with

$$\frac{\partial(\partial\Delta E/\partial q)}{\partial(1/r)} = \frac{6}{5} = 1.2 \qquad (12)$$

The agreement is quite good considering the latter value corresponds to uniform charge distributions, whereas charge distributions in atoms are not uniform, and the ionization process involves removing an electron from a small inner core at the center of the sphere.

The behavior of the intercepts, $E_{0,\alpha}$ in eq 7, is also of interest for interpreting simple potential models. The intercepts occur for mean dipole moment derivatives or GAPT charges that are zero. This corresponds to the core ionization energy of a neutral

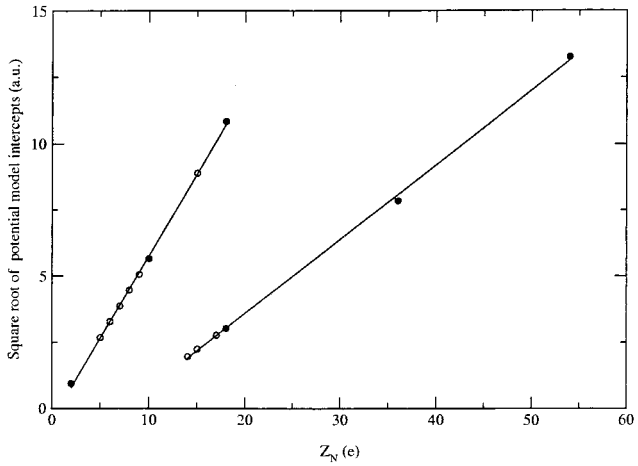

Figure 8. Square root of potential model intercepts graphed against nuclear charge. Experimental values (1s ionization energies of He, Ne, and Ar are 24.59, 869.07, and 3204.4 eV and the 2p ionization energies of Ar, Kr, and Xe are 247.64, 1676.85, and 4783.4 eV[1]) are represented by the darkened circles, whereas the white circles represent potential model intercepts.

atom. As such, the square roots of the intercepts are expected to be linearly related to the nuclear charges. In Figure 8, the square roots of the intercepts of the potential models obtained using only experimental core ionization energies and mean dipole moment derivatives are graphed against the nuclear charge. The linear plots shown there resemble the well-known Moseley diagrams[37] for X-ray emission spectra. As expected, the 1s He, Ne, and Ar and 2p Ar, Kr, and Xe ionization energies are found to fall nicely on the regression lines. However, the potential model intercept graph, contrary to the one for the slopes, is not a very sensitive one for testing this interpretation of the intercepts, because the different chemical environments cause small changes in the core ionization energy values. The nuclear charge variations account for almost all of the variance in the ordinate values in Figure 8.

Conclusion

It is indeed remarkable that the simple potential model is so successful in correlating energies obtained from X-ray spectroscopy and mean dipole moment derivatives obtained from infrared spectroscopy. The potential model results suggest that mean dipole moment derivatives can be interpreted as atomic charges in molecules. This is not the first real evidence, however, that atomic mean dipole moment derivatives are useful as atomic charges. Some years ago, Sambe[38] and later Lazzaretti and Zanasi[39] showed that the atomic polar tensor, of which the atomic mean dipole moment derivative is the trace, is simply related to the nuclear electric shielding tensor. As such, the force exerted on an atom of a molecule placed in an external electric field is directly related to its atomic polar tensor. So it should not be so surprising that the average of the diagonal elements of this tensor shows behavior expected for an atomic charge.

Acknowledgment. The authors are grateful to FAPESP and CNPq for partial financial support. R.L.A.H. thanks FAPESP, and A.E.O. thanks CNPq for doctoral fellowships. Some of the computer time consumed was graciously furnished by CENAPAD/SP.

References and Notes

(1) Siegbahn, K.; Nordling, C.; Johansson, G.; Hedman, J.; Heden, P. F.; Hamrin, K.; Gelius, U.; Bergmark, T.; Werme, L. O.; Manne, R.; Baer, Y. *ESCA Applied to Free Molecules*; North-Holland: Amsterdam, 1969.

(2) Guadagnini, P. H.; de Oliveira, A. E.; Bruns, R. E.; Neto, B. B. *J. Am. Chem. Soc.* **1997**, *119*, 4224−4231.

(3) de Oliveira, A. E.; Guadagnini, P. H.; Custódio, R.; Bruns, R. E. *J. Phys. Chem.* **1998**, *102*, 4615−4622.

(4) Haiduke, R. L. A.; de Oliveira, A. E.; Bruns, R. E. *J. Electron Spectrosc. Relat. Phenom.* **2000**, *107*, 211−219.

(5) de Oliveira, A. E.; Guadagnini, P. H.; Haiduke, R. L. A.; Bruns, R. E. *J. Phys. Chem. A* **1999**, *103*, 4918−4924.

(6) de Oliveira, A. E.; Haiduke, R. L. A.; Bruns, R. E. *J. Phys. Chem. A* **2000**, *104*, 5320−5327.

(7) Cioslowski, J. *J. Am. Chem. Soc.* **1989**, *111*, 8333−8336.

(8) Jolly, W. D.; Bombem, K. D.; Eyerman, C. J. *At. Data Nucl. Data Tables* **1984**, *31*, 433−493.

(9) Bruns, R. E.; Bassi, A. B. M. S. *J. Chem. Phys.* **1976**, *64*, 3053−3056.

(10) Bassi, A. B. M. S.; Bruns, R. E. *J. Phys. Chem.* **1976**, *80*, 2768−2770.

(11) Bruns, R. E.; Bassi, A. B. M. S. *J. Chem. Phys.* **1978**, *68*, 5448−5450.

(12) Neto, B. B.; Ramos, M. N.; Bruns, R. E. *J. Chem. Phys.* **1986**, *85*, 4515−4523.

(13) Bruns, R. E.; Brown, R. E. *J. Chem. Phys.* **1978**, *68*, 880−885.

(14) Martins Fº, H. P.; Bruns, R. E. *Spectrochim. Acta Part A* **1997**, *53*, 2115−2128.

(15) Castiglioni, C.; Gussoni, M.; Zerbi, G. *J. Chem. Phys.* **1985**, *82*, 3534−3541.

(16) Bruns, R. E. *J. Chem. Phys.* **1976**, *64*, 3084−3085.

(17) Martins Fº, H. P.; de Oliveira, A. E.; Haiduke, R. L. A.; Bruns, R. E. *Spectrochim. Acta Part A* **2001**, *57*, 255−264.

(18) Hopper, M. J.; Overend, J.; Ramos, M. N.; Bassi, A. B. M. S.; Bruns, R. E. *J. Chem. Phys.* **1983**, *79*, 19−25.

(19) de Oliveira, A. E.; Bruns, R. E. *Spectrochim. Acta Part A* **1999**, *55*, 2215−2219.

(20) Person, W. B.; Brown, K. G.; Steele, D.; Peters, D. *J. Phys. Chem.* **1981**, *85*, 1998−2007.

(21) de Oliveira. A. E. Ph.D. Thesis, Universidade Estadual de Campinas, Campinas, Brazil, 1999.

(22) Kagel, R. O.; Powell, D. L.; Hopper, M. J.; Overend, J.; Ramos, M. N.; Bassi, A. B. M. S.; Bruns, R. E. *J. Phys. Chem.* **1984**, *88*, 521−526.

(23) Martins Fº, H. P.; Guadagnini, P. H. *J. Mol. Struct. (THEOCHEM)* **1999**, *464*, 171−182.

(24) Overend, J. In *Infrared Spectroscopy and Molecular Structure*; Davis, M., Ed.; Elsevier: New York, 1963; p 354, Chapter 10.

(25) Biarge, J. F.; Herranz, J.; Morcillo, J. *An. R. Soc. Esp. Fis. Quim.* **1961**, *A57*, 81.

(26) Person, W. B.; Newton, J. H. *J. Chem. Phys.* **1974**, *61*, 1040−1049.

(27) Wilson, E. B.; Decius, J. C.; Cross, P. C. *Molecular Vibrations*; McGraw-Hill: New York, 1955.

(28) Newton, J. H.; Person, W. B. *J. Chem. Phys.* **1976**, *64*, 3036−3049.

(29) Schmidt, M. W.; Baldridge, K. K.; Batz, J. A.; Elbert, S. T.; Gordon, M. S.; Jensen, J. H.; Koseki, S.; Matsunaga, N.; Nguyen, K. A.; Su, S. J.; Windus, T. L.; Dupuis, M.; Montgomery, J. A. *J. Comput. Chem.* **1993**, *14*, 1347−1363.

(30) Frish, M. J.; Trucks, G. W.; Schlegel, H. B.; Gill, P. M. W.; Johnson, B. G.; Robb, M. A.; Cheeseman, J. R.; Keith, T. A.; Petersson, G. A.; Montgomery, J. A.; Raghavachari, K.; Al-Laham, M. A.; Zakrzewski, V. G.; Ortiz, J. V.; Foresman, J. B.; Peng, C. Y.; Ayala, P. Y.; Wong, M. W.; Andres, J. L.; Replogle, E. S.; Gomperts, R.; Martin, R. L.; Fox, D. J.; Binkley, J. S.; Defrees, D. J.; Baker, J.; Stewart, J. P.; Head-Gordon, M.; Gonzalez, C.; Pople, J. A. *Gaussian 94*, revision D.2; Gaussian, Pittsburgh, PA, 1995.

(31) Lide, D. R. *CRC Handbook of Chemistry and Physics*, 78th ed.; CRC Press: New York, 1997−1998.

(32) Jolly, W. L.; Perry, W. B. *J. Am. Chem. Soc.* **1973**, *95*, 5442−5449.

(33) Chong, D. P.; Hu, C. *J. Chem. Phys.* **1998**, *108*, 8950−8956.

(34) Bagus, P. S.; Coolbaugh, D.; Kowalczyk, S. P.; Pacchioni, G.; Parmigiani, F. *J. Electron Spectrosc. Relat. Phenom.* **1990**, *51*, 69−74.

(35) Pauling, L. *The Nature of the Chemical Bond*, 3th ed.; Cornell University Press: New York, 1960.

(36) Feynman, R. P.; Leighton, R. B.; Sands, M. *The Feynman Lectures on Physics*; Addison-Wesley: Reading, MA, 1969; pp 8−1.

(37) Semat, H. *Introduction to Atomic and Nuclear Physics*; Reinhart and Company, Inc.: New York, 1954.

(38) Sambe, H. *J. Chem. Phys.* **1973**, *58*, 4779−4782.

(39) Lazzaretti, P.; Zanasi, R. *J. Chem. Phys.* **1985**, *83*, 1218−1222. Lazzaretti, P.; Zanasi, R. *Chem. Phys. Lett.* **1984**, *112*, 103−105.